

## CALCULATION OF VELOCITY DISPERSION OF THE NEARBY GALAXIES USING DIFFERENT STELLAR TEMPLATE LIBRARIES

A. Lalović

*Astronomical Observatory, Volgina 7, 11060 Belgrade, Serbia*

E-mail: *ana@aob.rs*

(Received: February 8, 2010; Accepted: March 17, 2010)

**SUMMARY:** We present the central velocity dispersion measurements of the nearby galaxies from the Sloan Digital Sky Survey (SDSS). Using the sample from the paper by Ho et al. 2009, we have selected 23 galaxies for which we calculate the velocity dispersion. We have used the Penalized Pixel-Fitting code (Cappellari and Emsellem2004) to measure the velocity dispersion throughout the four chosen spectral regions: (3800,4568)Å, (4568,5336)Å, (5336,6104) and (6104,6872)Å. In all these regions, we have separately calculated dispersions and corresponding errors. We found that the measured values may vary with the change of spectral region, but, if weighted properly with the measure of the goodness of the fit, the final results will be shifted closer to those for the best fitting regions. We have also tested how the use of different spectral libraries (Miles, Valdes and Elodie databases) influences measurements and we showed that they do not affect measurements much. However, Elodie stellar library introduces the smallest errors in the velocity dispersion and it is the most stable throughout all four spectral regions. For these reasons it should be used preferentially when dealing with the SDSS spectra. We compare the results with the above mentioned paper and find a reasonable agreement. The agreement with the dispersions available in the HyperLeda database is very poor. The best agreement is obtained with SDSS measurements. We believe that our measurements are useful since SDSS velocity dispersions measurements are not available for many galaxies and the method of calculation of the velocity dispersion outlined in this work enables calculation of velocity dispersion for any galaxy. Of course, spectra with signal-to-noise ratio below 20 should be taken with caution.

**Key words.** Galaxies: bulges – Galaxies: kinematics and dynamics – Methods: numerical

### 1. INTRODUCTION

Accurate velocity dispersion measurements became a key point in our understanding of galaxies due to various correlations with other physical parameters. All scaling relations that depend on the velocity dispersion, particularly higher-order power law  $\sigma$ -relations, revealed the significance of accurate velocity dispersion measurements. The correlation between the maximum rotational velocity of the disk and the central stellar velocity dispersion of the bulge ( $v_m \sim \sigma_0$ ) offers insight into the relationship between

the halo and the bulge (Ho 2007). The well known Faber-Jackson relation (Faber and Jackson 1976), as well as the recently discovered tight correlation between stellar velocity dispersion and black hole mass (Ferrarese and Merritt 2000, Gebhardt et al. 2000), scale as the 4th order power law ( $M_{BH} \propto \sigma^4$ ), suggesting that small errors in velocity dispersion measurements produce large errors in these scaling relations. Bearing this in mind, we were driven to find the most insensitive way of measuring velocity dispersions using different spectral regions and stellar templates. Here, we present velocity dispersions for the nearby 23 galaxies in 4 different spectral regions

using 3 different stellar libraries and we calculate the velocity dispersion using stars of all spectral types, and of a combination of only G+K stars to find possible degeneracies. Finally, we perform an extensive analysis of various parameters that can influence velocity dispersion measurements and we made a comparison of kinematical parameters to the work of Ho et al. 2009 (Ho09). The outline of the paper is as follows: Section 2 describes the sample of galaxies used in this study, followed by a short description of the method in Section 3. In Section 4 we present different stellar libraries tested to obtain the one that best reconstructs the original galaxy spectra. In Section 5 we draw the conclusions.

## 2. THE SAMPLE OF GALAXIES

We have compiled a sample of 23 galaxies that make part of the Sloan Digital Sky Survey (SDSS) and are also present in Ho09 paper (*The Catalog Of Central Stellar Velocity Dispersions Of Nearby Galaxies*). This sample is chosen to be representative in a sense that it contains various morphological galaxy types (Fig 1). All the spectra are downloaded from the SDSS database according to their equatorial coordinates obtained using the electronic database HyperLeda (Paturel et al. 2003)<sup>1</sup> query form supplied with the catalogue names taken from Ho09. In the Ho09 paper, spectra came from the Palomar survey.

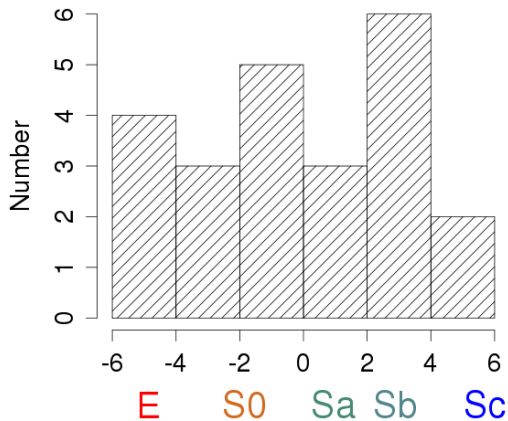


**Fig. 1.** Hubble type classification of our sample of galaxies.

Minimal signal-to-noise ratio in this sample is 10.43 and the median is 43.50. We have only 3 galaxies with signal-to-noise ratio  $S/N < 30$  (NGC 2770, NGC 4013 and NGC 4478).

## 3. LINE-OF-SIGHT VELOCITY DISTRIBUTION

For galaxies as stellar systems, the observed spectrum is a sum of individual stellar spectra originated in the stars moving with their line-of-sight velocities ( $v_{\text{los}}$ ) and redshifted to some spectral velocity  $u = c \ln \lambda$ . This shift of a spectral line  $\Delta\lambda = (v_{\text{los}}/c)\lambda$ , in terms of spectral velocity is simply the line-of-sight velocity:

$$\Delta u = c \frac{\Delta\lambda}{\lambda} \equiv v_{\text{los}}. \quad (1)$$

Based on the assumption that the spectrum of all stars is given by a single template  $S(u)$ , the galaxy spectrum  $G(u)$  is a convolution of the stellar spectrum and the line-of-sight velocity distribution function (LOSVD)  $F(v_{\text{los}})$ ,

$$G(u) \propto \int F(v_{\text{los}})S(u - v_{\text{los}})dv_{\text{los}}. \quad (2)$$

The LOSVD function can be retrieved by solving the inverse problem, i.e. deconvolving the spectra using the template. It can be modeled by using the sum of two Gaussians with different amplitudes (Rix and White 1992), means and dispersions. As a more general parametrization of the LOSVD, we can express the function in terms of its moments

$$\mu_k = \int (v_{\text{los}} - \bar{v}_{\text{los}})^k F(v_{\text{los}})dv_{\text{los}}. \quad (3)$$

By definition,  $\mu_1 = 0$  and the velocity dispersion ( $\sigma_{\text{los}}$ ) is simply the square root of the second moment  $\mu_2$  given as:

$$\mu_2 \equiv \sigma_{\text{los}}^2 = \int (v_{\text{los}} - \bar{v}_{\text{los}})^2 F(v_{\text{los}})dv_{\text{los}}. \quad (4)$$

But the higher-order moments reveal the shape of the LOSVD. They are often made dimensionless

$$\xi_k = \mu_k / \sigma_{\text{los}}^k \quad (5)$$

and they express the asymmetric (tail-like) and symmetric (bell-like) departures from the Gaussian usually denoted as the Gauss-Hermite parameters  $h_3$  and  $h_4$  (van der Marel and Franx 1993). We would have to know all the moments to determine the LOSVD function uniquely. In practice, however, if we have relatively low S/N-ratio of integrated spectra, we often assume the observed absorption line profiles to be Gaussian. In a subsequent paper (Samurović et al. 2010, in preparation), we will provide full kinematical profile, i.e. measured higher moments of the LOSVD function of galaxies extracted from SDSS. Here, we will restrict ourselves to Gaussian profiles, in order to compare our results obtained using 3 different stellar libraries to Ho09, HyperLeda database and existing SDSS measurements, which all assume a pure Gauss function.

<sup>1</sup><http://leda.univ-lyon1.fr/>

### 3.1. Direct Pixel Fitting method

Many techniques have been developed to recover LOSVD taking into account the signal-to-noise ratio and computational speed. Early methods mostly used Fourier-fitting technique since it provides a very quick way to recover LOSVD parameters, but more recent methods favour direct fitting in the pixel space. They require long calculation time, but have the advantage of easy exclusion of the gas emission lines.

Using extensive analysis made by Cappellari and Emsellem (2004), we have decided to use Penalized Pixel-Fitting (ppxf) code that operates in the pixel space<sup>2</sup>. We list some key points of this approach. In short, the best-fitting parameters of the LOSVD are determined by minimizing the  $\chi^2$  value, which measures the agreement between convolved stellar spectra and the LOSVD parametric function on the one hand, and galaxy spectrum on the other hand, over the set of good pixels using the BVLS procedure (Bounded-Variables Least-Squares algorithm by Lawson and Hanson 1995). It is very important to determine these good pixels, because a poor masking of bad pixels and emission lines introduces errors of up to 200%. This can easily be done by visual inspection since one pixel corresponds approximately to one angstrom in the case of the SDSS spectra. Table 3A. in the Appendix lists the emission lines masked prior to the fitting process.

Another important issue: if one is using thousand-angstrom scales, it is essential to normalize stellar spectra to unity and divide by a polynomial that fits the continuum, or else the  $\chi^2$  value will not be the true measure of the goodness of the fit. This can even influence the velocity dispersion measurements. To avoid this problem one may cut stellar spectra in intervals of several hundred angstroms, as is done here. For the same reason, we divide the galaxy spectrum by the average of the first and the last pixel value and multiplying it with some number so that the flux does not exceed 100 in any point. Also, the errors of the order  $\sim 10$  km/s may be obtained by leaving the code to determine the galaxy redshift. To avoid this problem, we previously deredshifted all galaxy spectra with MIDAS<sup>3</sup> using the redshifts found in the SDSS database. This preprocessing is essential to obtain good and stable results.

After the preparation is done, both the galaxy and the template spectra are rebinned in wavelength to a linear scale  $\ln \lambda$ , because shift of a spectral line corresponds to the line-of-sight velocity. Afterwards, template spectra are convolved with the quadratic difference between instrumental resolution of the object and template spectra in order to exclude nominal relative resolution difference (fifth column of Table 1). The bounded-variable least squares fitting is then applied between the galaxy spectrum and the stellar spectra that are previously convolved with the parametric Gauss-Hermite function (LOSVD) using

$h_3 = h_4 = 0$ . Template weights are simply least-squares coefficients of the fit, and they are not scaled in any way to yield the information on how they contribute to the galaxy spectrum. However, scaling the template spectra to unity prior to the fit reveals that some templates have higher absolute weights than others. We will return to this point in Sections 4 and 5.

## 4. FITTING PROCEDURE: THE KEY POINTS

There are two main points in the fitting process regardless of the method used. The first one is the so-called template mismatch problem. Namely, an assumption that there is the most "pronounced" star that can substitute various stellar types is essentially wrong, and may lead to very poor fitting results. This problem can be easily overcome nowadays by using numerous stellar libraries, that span over large wavelength ranges. However, there is still an issue whether these stars truly make the galaxy spectrum, or they are the source of some degeneracy. As we will show later, different parts of galaxy spectrum may favour different stellar types. This cannot be known a priori, but we have found that in the case with young stars, if the  $\chi^2$  value of the fit is better by an order of magnitude than in the case of G+K stars, the contribution of young stars is significant. Then, the error of the velocity dispersion compared to the error obtained using G+K stars will be approximately the same, contrary to the case when introduction of young stars only improves the fit through a slight decrease of the  $\chi^2$  value, but causes the increase in the velocity dispersion error for more than 100%. Then, even if the formal fit may appear better in the case of young stars, we should use G+K stars since these young stars do not contribute as G/K stars do.

The second point is a widely used assumption about the actual shape of the LOSVD function. For convenience, we assume that it can be well approximated by a Gaussian. In this way, we very often over(/under)estimate the velocity dispersion. On the other hand, when we have moderate quality spectra, this assumption is acceptable. Here, for the reasons of comparison, as mentioned earlier, we have used only pure Gaussians.

There is another issue of our lack of knowledge on how dispersion changes throughout the galaxy. The spectra of galaxies that are redshifted differ in the sense that the light is gathered using the fixed aperture (radius 1.5 arcsec in the case of SDSS spectra), thus the estimated velocity dispersions of more distant galaxies are affected by the motions of stars at larger galactocentric radii than for nearby galaxies. For example, if the velocity dispersion of galaxy decreases with radius, the estimated velocity dispersion (using a fixed aperture) of a more distant

<sup>2</sup><http://www-astro.physics.ox.ac.uk/mxc/idl/>

<sup>3</sup>ESO-MIDAS is a copyright protected software product of the European Southern Observatory, which provides general tools for image processing and data reduction.

**Table 1.** Description of stellar libraries used in this study. In the second and the third column the total number of stars is listed followed by the number of G and K stars. The fourth column contains the spectral coverage of libraries’ stellar spectra, and the fifth column contains the information on instrumental dispersion.

Library	No. stars	No. G and K stars	Spectral Range (Å)	Observational Resolution (km/s)
Miles	903	487	3525 - 7500	57
Valdes	654	371	3460 - 9464	22
Elodie	868	358	4100 - 6800	12

galaxy will be systematically smaller than the one of a similar galaxy nearby. This will result in a bias toward smaller velocity dispersions with redshift. However, due to the lack of long-slit spectra, we are forced to use these measurements bearing in mind that large scatter we often obtain, may in part be due to the fact that we use velocity dispersions measured at different radii.

#### 4.1. Stellar Libraries

We have used three stellar library databases (DBs), chosen to spread over (almost) the entire SDSS galaxy wavelength range. A basic description of the used libraries can be found in <http://www-astro.physics.ox.ac.uk/mxc/idl/>, with links to each database listed. Due to the limits imposed by the range of SDSS spectra (3800 – 7640)Å, we have chosen Miles (3525 – 7500)Å, Valdes (3460 – 9464)Å and Elodie (4100 – 6800)Å stellar libraries. A short description of libraries is given in Table 1. The last column in the table is the observational resolution. It is very important to incorporate it into the code, since it is a starting point for the fitting process. If omitted, or placed incorrectly, the fitting results will be very poor, if any. All stellar libraries yield similar results as will be shown below.

Another question is which stellar types to use for finding the optimal template. Apart from G+K stars, we have used all the stars available in the stellar libraries to measure velocity dispersions, and see how much young stars contribute to the galaxy spectra. Combination of G+K stars gives reasonably good fits with much smaller errors of the velocity dispersion than in the case when all stars were used. Introducing young stars improves the fit only formally – the  $\chi^2$  values are slightly smaller, but errors of the velocity dispersions are significantly larger than in the case of G+K stars. In Fig. 2, the difference between galaxy spectrum fitted using all template stars and only G+K stars from Elodie stellar library may be seen. The difference in velocity dispersion is about 60 km/s and the  $\chi^2$  value differ by order of magnitude larger. This was, however, the single case in our sample. In Fig. 3 we show a typical case of using young stars in addition to G+K stars, where the difference cannot be seen visually since the velocity dispersion changed by only 1 km/s, but the error of the velocity dispersion increased for 9 km/s. We have also tested the influence of change of the spectral re-

gions on the velocity dispersion measurements. We have found that the use of various spectral regions produces larger errors than inclusion of young stars, as will be shown in the next Subsection.

Using Elodie stellar library, we had only one galaxy which favored young stars, i.e. when both velocity dispersion error and the  $\chi^2$  value were improved by using young stars (Fig. 2). In all other cases, the velocity dispersion errors increased and the  $\chi^2$  values of the fit decreased slightly which implies some sort of degeneracy since the fit is performed using the template stars obtained through least-square fitting of all stars for each galaxy. The mixture of many stellar types results in the best-fitting template consisting of small amounts of all these stars (all stellar spectra are incorporated to some extent in the final template spectrum), understating the contribution of few stars that contribute most to the galaxy spectrum (the contribution of the most prominent stars is "masked" by other stars from the mixture). Thus, approximately the same values of the velocity dispersion and  $\chi^2$  of the fit imply that young stars do not contribute to galaxy spectrum as G and K stars do.

To summarize, the recipe for the successful determination of kinematical properties is to use only G+K stars, while for the galaxies with the  $\chi^2$  values significantly larger (order of magnitude) from others, one should introduce young stars in addition. If this, however, does not decrease the  $\chi^2$  value by an order of magnitude, than some other phenomenon is responsible for the poor result and the first fit (using G+K stars only) should be used, since some sort of degeneracy occurred.

#### 4.2. Tests with different spectral regions using all stellar libraries

We have initially divided the range covered by the SDSS spectra (3800,7640)Å in 5 parts, since this was the best solution to the slope-problem introduced in Subsection 3.1. However, the absence of any prominent absorption in the last part of the spectrum (6872,7399)Å<sup>4</sup> yielded very poor fit results, and we had to exclude this region. Finally, we formed 4 different regions: (3800,4568)Å, (4568,5336)Å, (5336,6104)Å and (6104,6872)Å. For each of them we have separately calculated the velocity dispersions using G+K stars and, in Fig. 5,

<sup>4</sup>Chosen also to coincide with the stellar libraries used and for this reason somewhat shorter.

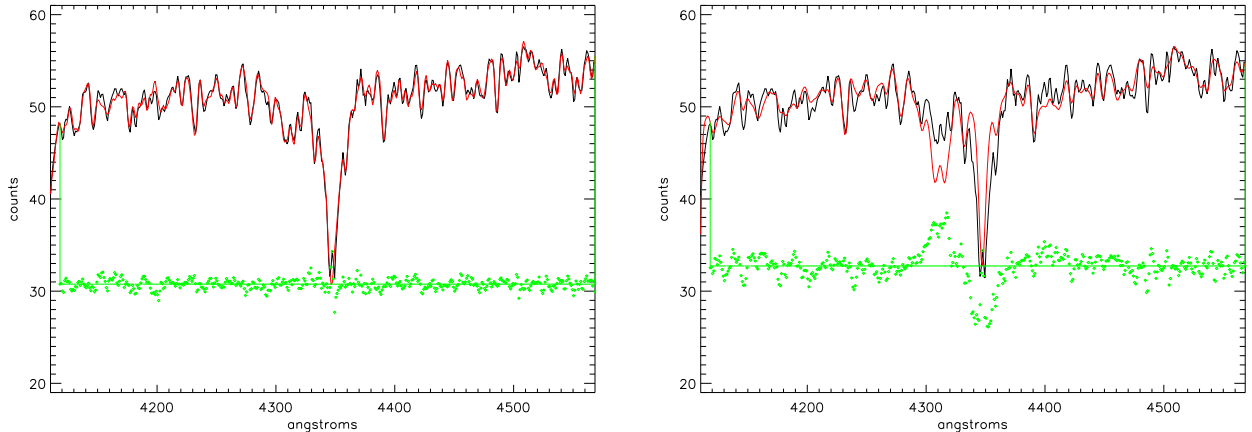


**Fig. 2.** (Left panel) Spectrum of NGC 3037 (black line) in the first region (see the text for the description of regions), using all stellar templates from Elodie stellar library yields  $\sigma = 56 \pm 1$  km/s, with  $\chi^2 = 0.3$  and A0 star as a dominant in the spectrum. Red line is the best-fit template star, and green dots at the bottom are residuals of the fit. (Right panel) The same galaxy using stellar templates of G and K stars; the velocity dispersion increased to  $\sigma = 121 \pm 4$  km/s, with  $\chi^2 = 1.4$  and G0 as a dominant star.

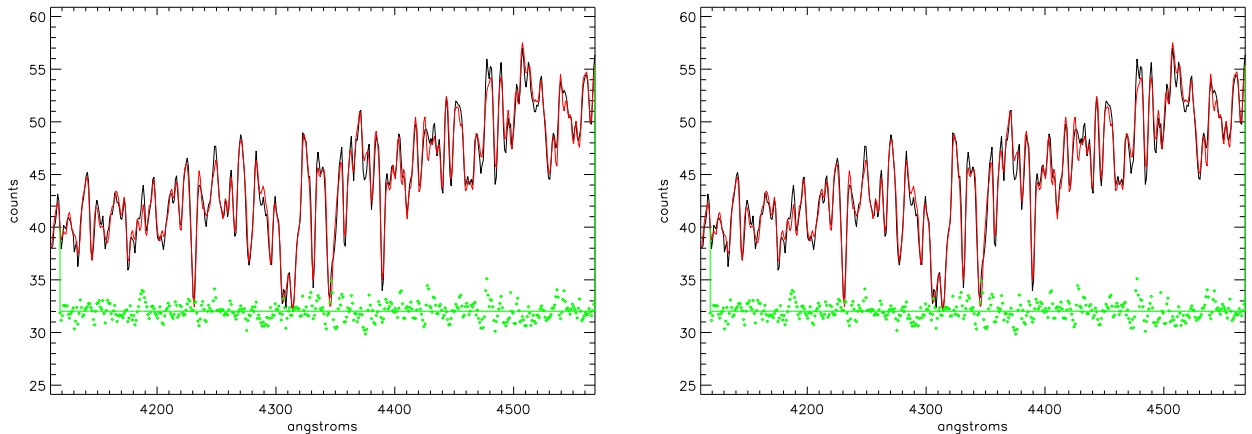


**Fig. 3.** (Left panel) Spectrum of NGC 4124 (black line) in the first region (see the text for the description of regions), using all stellar templates from Elodie stellar library, yields  $\sigma = 46 \pm 10$  km/s with  $\chi^2 = 0.67$  and F8I star as a dominant star in the spectrum. Red line is the best-fit template star, and green dots at the bottom are residuals of the fit. (Right panel) The same galaxy, but restricting stellar templates to G and K stars only, increases the velocity dispersion to  $\sigma = 47 \pm 1$  km/s with  $\chi^2 = 0.74$  and G0 as a dominant star.

we compare the results when different stellar libraries are used. In Fig. 5, velocity dispersion measurements from all 4 spectral regions are averaged according to Eq. (6) for all 3 stellar libraries used. One can see that Elodie database (Elodie DB in the legend) yields the smallest errors.

From the Fig. 4, one can conclude that Elodie database has the smallest errors of the velocity dispersion compared to other databases. Further, one may notice that the third region exhibits larger errors. These errors are much larger than those introduced by the usage of young stars in addition to G+K stars. To obtain a final value of the velocity dispersion, we have weighted both the velocity dispersion and its error from *each region* with its corre-

sponding  $\chi^2$ :

$$\bar{\sigma} = \frac{\sigma_1/\chi_1^2 + \sigma_2/\chi_2^2 + \sigma_3/\chi_3^2 + \sigma_4/\chi_4^2}{1/\chi_1^2 + 1/\chi_2^2 + 1/\chi_3^2 + 1/\chi_4^2} \quad (6)$$

$$\bar{\sigma}_{\text{err}} = \frac{\sigma_{1,\text{err}}/\chi_1^2 + \sigma_{2,\text{err}}/\chi_2^2 + \sigma_{3,\text{err}}/\chi_3^2 + \sigma_{4,\text{err}}/\chi_4^2}{1/\chi_1^2 + 1/\chi_2^2 + 1/\chi_3^2 + 1/\chi_4^2}, \quad (7)$$

where  $\bar{\sigma}$  is the average value of the velocity dispersion  $\sigma_i$  ( $i = 1, 2, 3, 4$ ) from all 4 spectral regions, weighted with  $\chi_i^2$  ( $i = 1, 2, 3, 4$ ) value of each region and  $\bar{\sigma}_{\text{err}}$  is the average value of the velocity dispersion error  $\sigma_{i,\text{err}}$  ( $i = 1, 2, 3, 4$ ) weighted in the same way.

The resulting values will be closer to those with the smaller  $\chi^2$  values, i.e. better fitted regions. The largest error from all 4 regions is taken as the final error of the velocity dispersion, even though

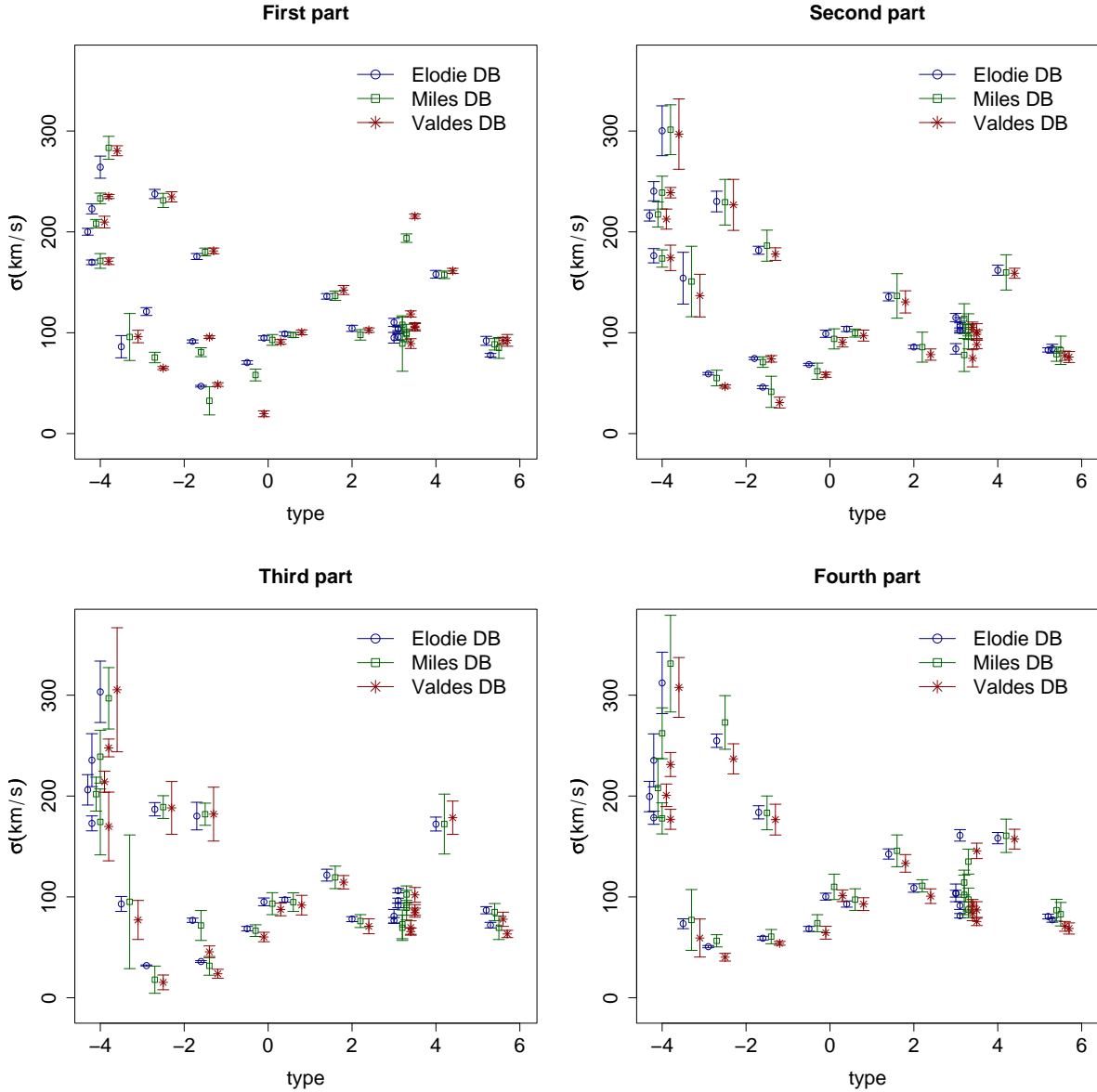


**Fig. 4.** The velocity dispersion measurements with corresponding errors in 4 different spectral regions for all 3 stellar databases used, as a function of Hubble type.

these are not real measurements (but fitting results) and errors are obtained using statistical methods. These errors are very similar to those given by Eq. (7) as can be seen from Fig. 6 (grey error bars correspond to the largest errors), where they are compared to somewhat smaller  $\chi^2$ -errors (black error bars). In Fig. 6 we compare the final results to the existing measurements from Ho09, HyperLeda and SDSS databases. Circles in Fig. 6 are averaged values (Eq. 6) of the velocity dispersion vs. Hubble type obtained using Elodie stellar library with gray error bars as the largest errors from all the regions and joined black error bars as errors weighted using Eq. (7).

Another comparison is made in Table 2, where results from the second ( $\sigma_{II}$ ) and the fourth ( $\sigma_{IV}$ ) region are compared to blue  $\sigma_{\text{blue}}$  and red  $\sigma_{\text{red}}$  part of the spectrum, taken from Ho09. There are differences that are not within errors, but the overall trend is the same. Regions do not overlap with those from Ho09 completely, which is in part responsible for the discrepancy. Namely, in Ho09 the so-called blue and red regions cover  $(4260, 4950)\text{\AA}$  and  $(6400, 6530)\text{\AA}$  respectively, while in this work the second region covers  $(4568, 5336)\text{\AA}$ , and the fourth  $(6104, 6872)\text{\AA}$ . The results differ and this cannot be explained by errors (errors do not span over the differences) or other stellar library used, since we have shown that different

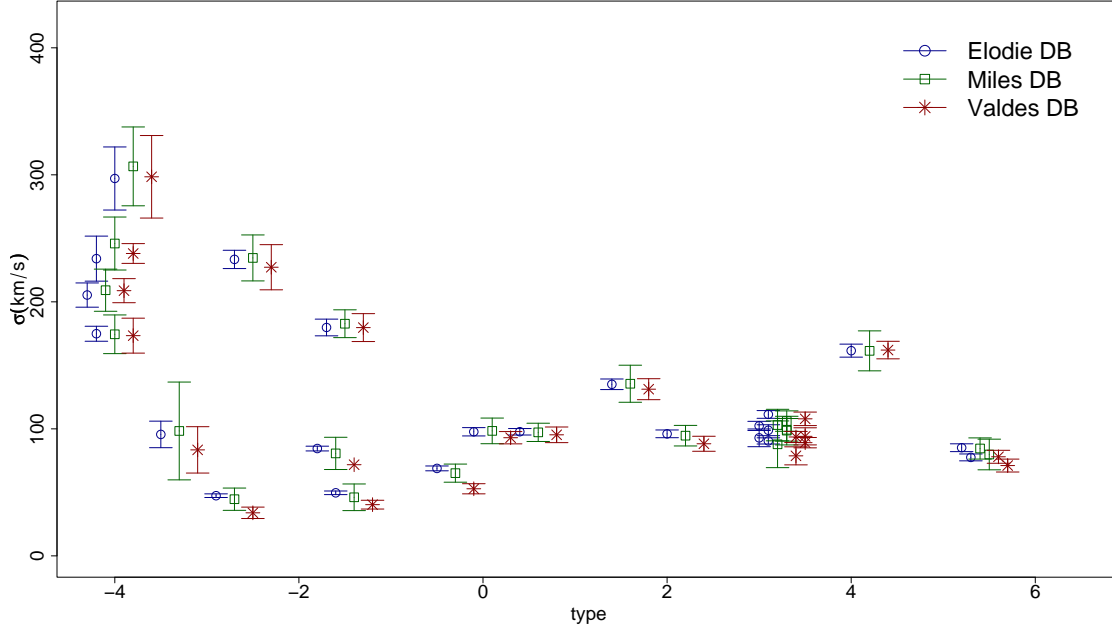


**Fig. 5.** The velocity dispersion of the sample of 23 galaxies as a function of the Hubble type for different stellar libraries. The results are mostly within errors calculated using the Monte-Carlo simulation of the noise added artificially to the stellar template spectra. There is a small offset along the  $x$ -axis for the reason of visual clarity. Points are calculated as weighted averages in 4 spectral regions according to Eq. (6). For error bars we have taken the largest error from all 4 regions for each galaxy.

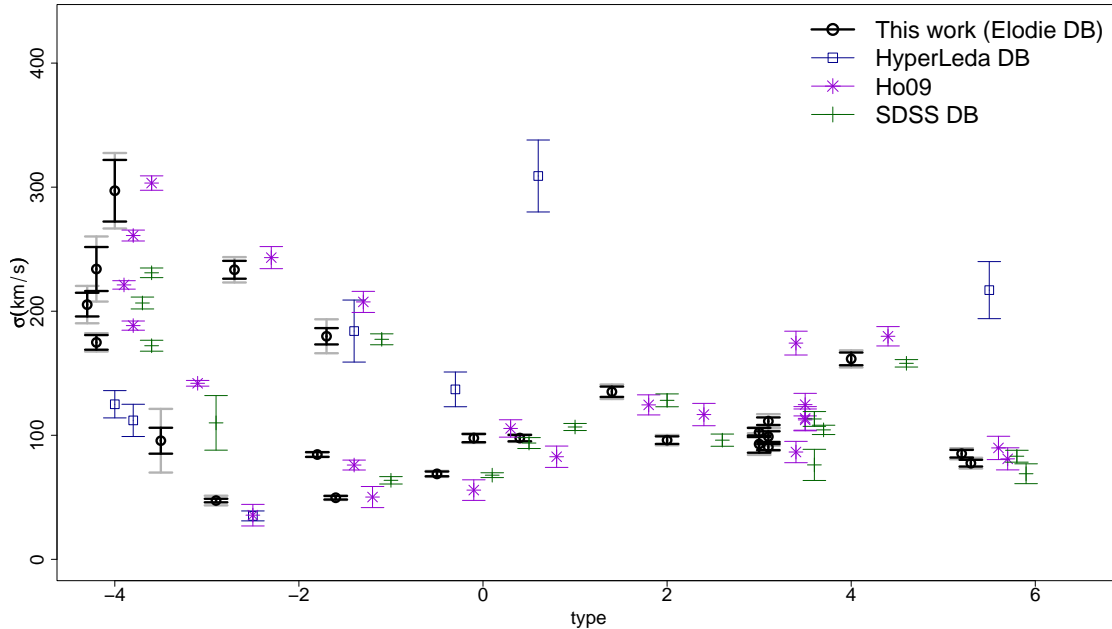


**Fig. 6.** Calculated velocity dispersions with weighted  $\chi^2$  errors (black) and largest errors from all 4 regions (gray) compared to the existing measurements listed in the legend as a function of the Hubble type.

**Table 2.** Comparison of the velocity dispersion measurements with Ho09. The results are compared in the second ( $\sigma_{II}$ ) and the fourth ( $\sigma_{IV}$ ) spectral region to the blue  $\sigma_{\text{blue}}$  and red  $\sigma_{\text{red}}$  part of the spectrum from Ho09. The so-called blue and red regions from Ho09 cover (4260,4950)Å and (6400,6530)Å respectively, while in this work the second region covers (4568,5336)Å, and the fourth (6104,6872)Å.

name	type	$\sigma_{\text{blue}}$ (km/s)	$\sigma_{II}$ (km/s)	$\sigma_{\text{red}}$ (km/s)	$\sigma_{IV}$ (km/s)
NGC2543	3.1	163.4 ± 20.8	102.18 ± 2.57	101.3 ± 9.7	81.29 ± 2.19
NGC2770	5.3	/ ± /	84.21 ± 4.33	81 ± 8.9	77.19 ± 2.26
NGC2911	-2.7	265.8 ± 16.1	230.12 ± 10.23	233.4 ± 10.6	254.84 ± 6.61
NGC3073	-2.9	/ ± /	59.38 ± 1.19	35.6 ± 8.7	50.68 ± 1.11
NGC3692	3.1	/ ± /	107.68 ± 7.32	113.6 ± 9.5	91.38 ± 3.83
NGC3780	5.2	/ ± /	82.93 ± 2.08	89.8 ± 9.4	80.54 ± 2.4
NGC4013	3	/ ± /	84.02 ± 5.19	86.5 ± 8.6	103.98 ± 8.76
NGC4102	3	162.9 ± 24.5	115.06 ± 4.06	176.4 ± 10.4	103.19 ± 3.38
NGC4124	-1.6	/ ± /	45.99 ± 1.49	50.2 ± 8.5	59.1 ± 1.82
NGC4168	-4.2	169.4 ± 13.3	176.36 ± 7.07	199.6 ± 10.2	178.45 ± 6.48
NGC4220	-0.1	133.3 ± 11.7	98.98 ± 3.53	90.1 ± 8.7	100.26 ± 3.43
NGC4245	0.4	/ ± /	103.72 ± 2.55	82.7 ± 8.6	92.9 ± 3.06
NGC4261	-4	311.6 ± 22.7	300.26 ± 24.72	301 ± 12	312.21 ± 30.43
NGC4421	-0.5	/ ± /	68.54 ± 1.1	55.8 ± 8.3	68.3 ± 2.43
NGC4478	-3.5	114.3 ± 11.3	154.09 ± 25.66	161.4 ± 9.5	73.39 ± 4.87
NGC4636	-4.3	219.8 ± 15.2	216.26 ± 5.51	221.9 ± 10.5	199.5 ± 15.06
NGC5273	-1.8	/ ± /	74.59 ± 1.22	76 ± 8.8	334.21 ± 2.09
NGC5371	4	187.4 ± 13.3	161.99 ± 4.98	175.7 ± 9.7	158.27 ± 5.61
NGC5448	1.4	121.4 ± 14.9	135.67 ± 4.06	125.8 ± 9.7	142.55 ± 5.04
NGC5485	-1.7	179.2 ± 14.6	181.78 ± 3.98	221.8 ± 10.4	183.84 ± 6.53
NGC5656	2	/ ± /	85.82 ± 1.82	116.7 ± 9	108.75 ± 4.15
NGC5806	3.1	/ ± /	106 ± 3.81	124.7 ± 9.1	161.01 ± 5.7
NGC5846	-4.2	225.3 ± 15.8	240.3 ± 9.52	276.2 ± 10.3	235.41 ± 26.24

stellar libraries cause only small differences both regarding dispersions and corresponding errors. We have calculated dispersions using the same stellar library (with only G and K stars) as in Ho09 and, again, we could not find better agreement (Table 2A in the Appendix). We are left with only one conclusion – the code is responsible for the differences.

In Table 3, we have listed measurements from Ho09 ( $\sigma_{\text{Ho09}}$ ), HyperLeda database ( $\sigma_{\text{Leda}}$ ), SDSS database ( $\sigma_{\text{SDSS}}$ ) and those derived in this work ( $\sigma_{\text{final}}$ ). To obtain a single value from the HyperLeda database  $\sigma_{\text{Leda}}$ , we have calculated averaged values weighting dispersions from all given catalogues with the corresponding errors, if given. If the errors were not supplied or some values differed significantly, we have omitted those measurements. We have taken the largest error from all measurements for each galaxy. The last column in the table ( $\sigma_{\text{final}}$ ) is the averaged velocity dispersion weighted using Eq. (6) and the errors are the largest errors from all four spectral regions, which correspond to gray error bars in Fig. 6. To obtain this  $\sigma_{\text{final}}$ , we have used the Elodie database since we found it is the most reliable, and stable when young stars are introduced; the results are insensitive to the morphological type of galaxies and they are very stable throughout the spectral regions used.

We have found a very good agreement with SDSS DB measurements, reasonable agreement with Ho09 values and large discrepancies when we compare our results with the data found in the HyperLeda database. However, HyperLeda is a compilation of catalogues and the results found there are averaged values from several catalogues.

## 5. CONCLUSIONS

We have calculated central velocity dispersions for 23 nearby galaxies from the SDSS survey, that are also included in the paper by Ho et al. 2009 (Ho09), where galaxy spectra from Palomar survey had been used. In this sample of galaxies all morphological types are represented. Galaxy stellar kinematics was extracted from the absorption-line spectra using Penalized Pixel-Fitting method (Cappellari and Emsellem 2004). In this study we have divided the galaxy spectrum in four regions to be able to obtain reliable and comparable estimates of the goodness of the fit, since the existing slope in the stellar templates spectra affects this value. The second and the fourth region approximately coincide with the so-called blue and red spectrum from the paper Ho09. We have found reasonable agreement with the velocity dispersion measurements from the paper Ho09 (Table 2).



**Table 3.** Comparison of velocity dispersion measurements with those from Ho09 paper ( $\sigma_{\text{Ho09}}$ ), HyperLeda database ( $\sigma_{\text{Leda}}$ ), SDSS database ( $\sigma_{\text{SDSS}}$ ) and this work ( $\sigma_{\text{final}}$ ).

galaxy	$\sigma_{\text{Ho09}}$ (km/s)	$\sigma_{\text{Leda}}$ (km/s)	$\sigma_{\text{SDSS}}$ (km/s)	$\sigma_{\text{final}}$ (km/s)
NGC2543	112.4 ± 8.8	/	/	90.49 ± 3.08
NGC2770	81 ± 8.9	217 ± 23	69 ± 8	77.52 ± 4.33
NGC2911	243.2 ± 8.9	35 ± 4	/	233.39 ± 10.23
NGC3073	35.6 ± 8.7	/	/	47.38 ± 3.89
NGC3692	113.6 ± 9.5	/	/	98.92 ± 7.32
NGC3780	89.8 ± 9.4	/	83.11 ± 4.79	85.15 ± 4.44
NGC4013	86.5 ± 8.6	/	76.12 ± 12.56	92.92 ± 8.76
NGC4102	174.3 ± 9.6	/	113.15 ± 5.96	102.32 ± 4.06
NGC4124	50.2 ± 8.5	184 ± 25	63.69 ± 2.98	49.65 ± 1.82
NGC4168	188.4 ± 8.1	125 ± 11	172.18 ± 4.4	174.87 ± 7.39
NGC4220	105.5 ± 7	/	93.73 ± 4.4	97.69 ± 3.87
NGC4245	82.7 ± 8.6	309 ± 29	106.68 ± 2.85	97.7 ± 3.06
NGC4261	303.3 ± 10.6	112 ± 13	/	297.11 ± 30.43
NGC4421	55.8 ± 8.3	137 ± 14	67.84 ± 1.94	68.87 ± 2.43
NGC4478	141.9 ± 7.3	/	110 ± 22	95.61 ± 25.66
NGC4636	221.2 ± 8.6	/	206.62 ± 4.79	205.33 ± 15.06
NGC5273	76 ± 8.8	/	/	84.48 ± 2.09
NGC5371	179.8 ± 7.8	/	158 ± 3	161.57 ± 6.9
NGC5448	124.5 ± 8.1	/	128.17 ± 5.18	135.09 ± 5.86
NGC5485	207.5 ± 8.5	/	177.36 ± 4.4	179.81 ± 13.68
NGC5656	116.7 ± 9	/	96.06 ± 4.92	96.07 ± 4.15
NGC5806	124.7 ± 9.1	/	104.35 ± 3.75	111.34 ± 5.7
NGC5846	261 ± 8.6	/	230.96 ± 3.88	234.01 ± 26.24

We have tested three stellar libraries: Miles, Valdes and Elodie and found that Elodie database is the best for dealing with SDSS spectra. Apart from the fact that it produces the smallest errors of the velocity dispersion, it is also insensitive to the morphological type of galaxies used and errors do not scale with  $\chi^2$  of the fit (as is expected) since errors are obtained using statistical method *after* the best-fit template is calculated. We believe that weighting of the velocity dispersion should be done using  $\chi^2$  of the fit instead of errors since it is the only parameter that is calculated together with the optimal template in the fitting process. Considering errors, it seems the most appropriate to take the largest error from all fitted regions. Weighting errors with  $\chi^2$  is not appropriate for the same reason (velocity dispersions and errors are not calculated simultaneously). However, differences are very small and formal errors calculated in both ways can be used (difference between black and grey error bars in Fig. 6). As we have mentioned earlier, there is no point in taking the lower and upper limit within regions for the error, since the averaged value is shifted toward smaller  $\chi^2$  regions so that the error can not encompass the velocity dispersion measurements from all four regions. Moreover, this shifting enables better measurements (with smaller  $\chi^2$  values), to contribute more to the final averaged dispersion, so even if the dispersion is quite different in some spectral region and less precisely determined (with larger  $\chi^2$  value) it will not

much affect this final, adopted value. It is, therefore, important to use the *whole* galaxy spectrum for determination of the velocity dispersion.

The main reason for the discrepancy between different spectral regions is a bad masking of the emission lines. It may change the calculated dispersion by even more than 200%. This is the reason why we give the list of the masked lines in the Appendix (Table 3A). Another reason could be the use of only G and K stars to obtain the optimal template star. We have given the example of one star (Fig. 2) where there is a real need of adding young stars in addition to G and K stars. In all cases except this one, we have shown that young stars do not contribute to the galaxy spectra and are responsible for enlarging the errors of the velocity dispersion.

Finally, we made a comparison with the measurements from Ho09 paper, Hyperleda and SDSS database (Fig. 6). We have good agreement with the results from the SDSS survey, and we believe this is due to the fact that in SDSS the whole galaxy spectrum is used in the fitting process. We obtained a reasonable agreement with Ho09 measurements, but there are differences that cannot be explained by differences in the spectral regions or stellar library used only. As can be seen from Table 1A in the Appendix, the velocity dispersion does not change much throughout the spectral regions; we have also calculated dispersions of the sample using Valdes stellar library (Appendix: Table 2A) and, again, could not find a better agreement with Ho09 paper. We believe

this discrepancy may be due to the different code used. SDSS velocity dispersions are calculated also with a different code, but there is a good agreement with our work. Large discrepancies with HyperLeda catalogue measurements probably come from the fact that it is the compilation of catalogues.

*Acknowledgements* – This work was supported by the Ministry of Science and Technological Development of the Republic of Serbia through the project no. 146012, "Gaseous and Stellar Component of the Galaxy: Interaction and Evolution". The author is grateful to Srdjan Samurović for helpful discussions. The author acknowledges the usage of the SDSS database (<http://cas.sdss.org/astrodr7/en/>) and the usage of the HyperLeda database (<http://leda.univ-lyon1.fr>). The author also acknowledges the usage of the Penalized Pixel-Fitting code, developed by Michele Cappellari (<http://www-astro.physics.ox.ac.uk/mxc/idl/>).

## REFERENCES

- Cappellari, M., Emsellem, E.: 2004 *Publ. Astron. Soc. Pacific*, **116**, 138.
- Faber, S. M., Jackson, R. E.: 1976, *Astrophys. J.*, **204**, 668.
- Ferrarese, L., Merritt, D.: 2000, *Astrophys. J.*, **539**, 9.
- Gebhardt, K., Bender, R., Bower, G. et al.: 2000, *Astrophys. J.*, **539**, 13.
- Ho, L. C., Greene, J. E., Filippenko, A. V., Sargent, W. L. W.: 2009, *Astrophys. J. Suppl. Series*, **183**, 1.
- Ho, L. C.: 2007, *Astrophys. J.*, **668**, 94.
- Lawson, C., Hanson, R.: Solving Least Squares Problems, Revised edition, 1995. SIAM, 1995, ISBN: 0898713560, LC: QA275.L38.
- Paturel, G., Petit, C., Prugniel, Ph., Theureau, G., Rousseau, J., Brouty, M., Dubois, P., Cambresy, L.: 2003, *Astron. Astrophys.*, **412**, 45.
- Rix, H.-W., White, S. D. M.: 1992 *Mon. Not. R. Astron. Soc.*, **254**, 389.
- Samurović, S. et al.: 2010, in preparation.
- van der Marel, R. P., Franx, M.: 1993 *Astrophys. J.*, **407**, 525.

## APPENDIX

**Table 1A.** Velocity dispersion measurements in all 4 spectral regions using Elodie stellar library. For each region covering (3800,4568) Å, (4568,5336) Å, (5336,6104) Å and (6104,6872) Å, respectively we have calculated velocity dispersion ( $\sigma_1$ ,  $\sigma_2$ ,  $\sigma_3$  and  $\sigma_4$ ). We also list  $\chi^2$  values of the fit in each spectral region ( $\chi_1^2$ ,  $\chi_2^2$ ,  $\chi_3^2$  and  $\chi_4^2$ ).

name	type	$\sigma_1$ (km/s)	$\chi_1^2$	$\sigma_2$ (km/s)	$\chi_2^2$	$\sigma_3$ (km/s)	$\chi_3^2$	$\sigma_4$ (km/s)	$\chi_4^2$	$\sigma_{final}$ (km/s)
NGC2543	3.1	95.76 ± 3.08	0.06	102.18 ± 2.57	0.02	91.64 ± 2.36	0.06	81.29 ± 2.19	0.02	90.49 ± 3.08
NGC2770	5.3	77.7 ± 1.79	0.4	84.21 ± 4.33	0.29	72.02 ± 2.79	0.27	77.19 ± 2.26	0.12	77.52 ± 4.33
NGC2911	-2.7	237.58 ± 4.56	0.14	230.12 ± 10.23	0.13	186.92 ± 6.61	0.4	254.84 ± 6.61	0.19	233.39 ± 10.23
NGC3073	-2.9	56.26 ± 1.13	0.31	59.38 ± 1.19	0.37	31.99 ± 0.51	0.18	50.68 ± 1.11	0.14	47.39 ± 3.89
NGC3692	3.1	103.9 ± 3.62	0.64	107.68 ± 7.32	0.65	96.24 ± 2.51	0.7	91.38 ± 3.83	0.43	98.92 ± 7.32
NGC3780	5.2	91.98 ± 4.44	1.1	82.93 ± 2.08	1.05	86.79 ± 3.55	0.77	80.54 ± 2.4	0.74	85.15 ± 4.44
NGC4013	3.0	95.03 ± 5.3	3.86	84.02 ± 5.19	2.84	80.83 ± 6.71	2.6	103.98 ± 8.76	1.53	92.92 ± 8.76
NGC4102	3.0	110.24 ± 4.03	0.42	115.06 ± 4.06	0.31	76.68 ± 2.89	0.41	103.19 ± 3.38	0.29	102.32 ± 4.06
NGC4124	-1.6	46.98 ± 0.84	0.74	45.99 ± 1.49	0.39	35.9 ± 0.87	0.44	59.1 ± 1.82	0.21	49.65 ± 1.82
NGC4168	-4.2	169.83 ± 2.3	0.51	176.36 ± 7.07	0.42	172.89 ± 7.39	0.54	178.45 ± 6.48	0.35	174.87 ± 7.39
NGC4220	-0.1	94.8 ± 2.09	0.43	98.98 ± 3.53	0.31	95.08 ± 3.87	0.43	100.26 ± 3.43	0.3	97.69 ± 3.87
NGC4245	0.4	98.91 ± 2.08	0.48	103.72 ± 2.55	0.5	97.16 ± 2.41	0.32	92.9 ± 3.06	0.37	97.7 ± 3.06
NGC4261	-4.0	264.17 ± 10.96	0.64	300.26 ± 24.72	0.57	303.34 ± 30.43	0.67	312.21 ± 30.43	0.41	297.11 ± 30.43
NGC4421	-0.5	70.55 ± 1.71	0.83	68.54 ± 1.1	0.69	68.49 ± 2.21	0.7	68.3 ± 2.43	0.56	68.87 ± 2.43
NGC4478	-3.5	86.18 ± 11.02	6.59	154.09 ± 25.66	4.7	93.01 ± 7.4	4.26	73.39 ± 4.87	2.14	95.61 ± 25.66
NGC4636	-4.3	200.13 ± 3.38	0.39	216.26 ± 5.51	0.43	206.15 ± 15.06	0.45	199.5 ± 15.06	0.42	205.33 ± 15.06
NGC5273	-1.8	91.37 ± 1.49	0.05	74.59 ± 1.22	0.13	76.85 ± 2.09	0.02	334.21 ± 2.09	0.68	84.48 ± 2.09
NGC5371	4.0	157.98 ± 3.84	0.14	161.99 ± 4.98	0.14	172.24 ± 6.9	0.25	158.27 ± 5.61	0.16	161.57 ± 6.9
NGC5448	1.4	136.07 ± 2.76	0.22	135.67 ± 4.06	0.22	121.57 ± 5.86	0.43	142.55 ± 5.04	0.31	135.09 ± 5.86
NGC5485	-1.7	175.56 ± 2.98	0.41	181.78 ± 3.98	0.51	180.12 ± 13.68	0.51	183.84 ± 6.53	0.68	179.81 ± 13.68
NGC5656	2.0	104.37 ± 3.04	1.07	85.82 ± 1.82	1.01	77.98 ± 2.46	0.99	108.75 ± 4.15	0.62	96.07 ± 4.15
NGC5806	3.1	103.9 ± 1.82	0.36	106 ± 3.81	0.28	106.23 ± 2.17	0.42	161.01 ± 5.7	0.95	111.34 ± 5.7
NGC5846	-4.2	222.8 ± 4.91	0.45	240.3 ± 9.52	0.39	235.57 ± 26.24	0.34	235.41 ± 26.24	0.35	234.01 ± 26.24

**Table 2A.** Here, we compare velocity dispersion measurements with the paper Ho09 using the same stellar library Valdes. In the paper Ho09 the spectral range was divided in two regions, the so-called blue (4260,4950)Å and red region (6400,6530)Å. These two regions are marked as  $\sigma_{\text{blue}}$  and  $\sigma_{\text{red}}$  in Table 2. They are compared to the second (4568,5336)Å and the fourth region (6104,6872)Å of this work ( $\sigma_{II}$  and  $\sigma_{IV}$ ). There are differences that are not within errors, but the agreement is well.

name	$\sigma_{\text{blue}}$ (km/s)	$\sigma_{II}$ (km/s)	$\sigma_{\text{red}}$ (km/s)	$\sigma_{IV}$ (km/s)
NGC2543	163.4 ± 20.8	95.93 ± 11.97	101.3 ± 9.7	87.29 ± 7.91
NGC2770	/	82.56 ± 14.05	81 ± 8.9	82.84 ± 11.63
NGC2911	265.8 ± 16.1	229.43 ± 22.62	233.4 ± 10.6	272.96 ± 26.59
NGC3073	/	55.07 ± 7.75	35.6 ± 8.7	56.47 ± 6.05
NGC3692	/	106.05 ± 12.73	113.6 ± 9.5	97.44 ± 11.35
NGC3780	/	78.77 ± 7.04	89.8 ± 9.4	86.83 ± 10.76
NGC4013	/	77.97 ± 16.38	86.5 ± 8.6	102.03 ± 19.62
NGC4102	162.9 ± 24.5	113.99 ± 14.77	176.4 ± 10.4	114.22 ± 12.28
NGC4124	/	41.44 ± 15.45	50.2 ± 8.5	60.62 ± 7.06
NGC4168	169.4 ± 13.3	173.59 ± 8.58	199.6 ± 10.2	177.85 ± 15.41
NGC4220	133.3 ± 11.7	93.92 ± 9.98	90.1 ± 8.7	109.97 ± 12.6
NGC4245	/	99.69 ± 3.98	82.7 ± 8.6	97.33 ± 10.72
NGC4261	311.6 ± 22.7	301.31 ± 24.72	301 ± 12	331.29 ± 47.94
NGC4421	/	61.85 ± 8.03	55.8 ± 8.3	73.92 ± 8.46
NGC4478	114.3 ± 11.3	150.81 ± 34.94	161.4 ± 9.5	77.13 ± 30.17
NGC4636	219.8 ± 15.2	217.3 ± 12.42	221.9 ± 10.5	207.94 ± 29.26
NGC5273	/	70.9 ± 5.22	76 ± 8.8	449.56 ± 14.82
NGC5371	187.4 ± 13.3	159.82 ± 17.48	175.7 ± 9.7	160.59 ± 16.52
NGC5448	121.4 ± 14.9	136.5 ± 22.06	125.8 ± 9.7	145.68 ± 15.76
NGC5485	179.2 ± 14.6	186.33 ± 15.4	221.8 ± 10.4	183.31 ± 16.76
NGC5656	/	85.73 ± 14.87	116.7 ± 9	110.95 ± 6.07
NGC5806	/	102.62 ± 5.81	124.7 ± 9.1	135.01 ± 12.37
NGC5846	225.3 ± 15.8	238.97 ± 16.29	276.2 ± 10.3	262.21 ± 25.22

**Table 3A.** The list of the masked spectral lines used in the fitting process along with the corresponding widths.

Line (Å)	4861.3	4958.9	5006.9	5150	5200	5610	5756	5560
Width (km/s)	800	500	800	400	300	250	500	400
Line (Å)	6300	6410	6340	6570	6720	6795	7012	7320
Width (km/s)	400	200	400	1600	900	400	400	200

**ОДРЕЂИВАЊЕ ДИСПЕРЗИЈЕ БРЗИНА БЛИСКИХ ГАЛАКСИЈА  
КОРИШЋЕЊЕМ РАЗЛИЧИТИХ БИБЛИОТЕКА ЗВЕЗДАНИХ СПЕКТАРА****A. Lalović***Astronomical Observatory Belgrade, Volgina 7, 11060 Belgrade, Serbia*E-mail: *ana@aob.rs*

УДК 524.7–325–17

*Оригинални научни рад*

Представљамо мерења дисперзија радијалних брзина блиских галаксија из Sloan Digital Survey-а (SDSS). Користећи узорак галаксија из рада Ho et al. 2009, изабрали смо 23 галаксије за које смо израчунали дисперзије брзина. У овом раду коришћен је програм "Penalized Pixel Fitting" (Cappellari and Emsellem 2004) за одређивање дисперзија у четири одабрана спектрална подручја:  $(3800,4568)\text{\AA}$ ,  $(4568,5336)\text{\AA}$ ,  $(5336,6104)$  и  $(6104,6872)\text{\AA}$ . У свим овим областима, независно је одређена дисперзија са одговарајућом грешком. Установили смо да се мерење вредности мењају са променом спектралне области, али уколико се отежају са мером успешности фита, крајњи резултати биће померени ка најбоље израчунатим вредностима. Такође, тестирали смо како различите библиотеке звезданих спектра (Miles, Valdes и Elodie базе спек-

тара) утичу на мерења и показали да је тај утицај занемарљив. Ипак, употреба Elodie звезданих спектра даје најмању грешку дисперзије брзина и најстабилнија је кроз све четири области спектра и из ових разлога сматрамо да је најбоље користити је за SDSS спектре. Резултати се добро слажу са поменути радом (Хо и сарадници 2009). Са друге стране, слагање са мерењима дисперзија брзина доступних у бази HyperLeda је веома лоше. Најбоље слагање је остварено са мерењима доступним у SDSS бази података. Верујемо да су наша мерења потребна из разлога што дисперзије брзина недостају у SDSS бази за велики број галаксија и зато што коришћени метод даје резултате за све галаксије. Ипак, резултате за галаксије са односом сигнала према шуму испод 20 треба узимати са опрезом.